Performance Analysis of Distributed Beamforming in Wireless Networks: The Effect of Synchronization and Doppler spread

Ioannis Dagres
National and Kapodistrian University of Athens, Greece
jdagres@phys.uoa.gr

Andreas Polydoros
National and Kapodistrian University of Athens, Greece
apolydoros@phys.uoa.gr

Aris Moustakas
National and Kapodistrian University of Athens, Greece
arislm@phys.uoa.gr

MILCOM 2021 - 2021 IEEE Military Communications Conference (MILCOM) | 978-1-6654-3956-5/21/$31.00 ©2021 IEEE | DOI: 10.1109/MILCOM52596.2021.9653042

***Abstract*—Distributed Beam-Forming (DBF) is a promising technique for increasing range and throughput in cooperative wireless networks. It is known, however, that DBF is sensitive to carrier-synchronization ("synch") errors among the spatially separated RF oscillators in the distinct transmitting radios as well as errors due to independently occurring Doppler spread (fading) in each contributing link. We analyze here the statistical behavior of the resulting time-dependent beamforming gain as a function of these synch errors and dynamics-induced Doppler spread. A Gamma-distribution approximation is employed and compared to simulation for the resulting gains and system performance. The proposed statistics can subsequently be employed for optimizing the design parameters of a DBF protocol (frame period, pilot length, resynch period) for given pre-specified capacity or link-outage constraints.**

Keywords—distributed, beamforming, synchronization errors, Doppler spread, gain outage.

I. INTRODUCTION

Network-node synchronization ("synch") has long been recognized as an important problem for all types of networks [1]. Lack of ideal (perfect) carrier synch among the node-owned, distributed RF oscillators exists regardless of whether an open-loop or closed-loop (master-slave) network architecture is adopted, although obviously the quality of the synch depends on the architecture (cf. [7]). However, the more recent paradigm of distributed wireless-sensor-network radio nodes attempting to cooperatively beam-form to a remote destination, denoted as Distributed Beam-Forming (DBF), has imposed new demands on this old synch problem [2-5], although unsynchronized versions for low-power, low-cost applications have also been developed [6]. In addition to the challenge of synchronization, distributed beamforming is particularly vulnerable to independent (per-link) channel variations, which degrade the degree of coherence between nodes over time. This paper addresses the performance impact of simultaneous imperfect synch plus channel dynamics.

In standard point-to-point links, carrier synch is achieved via dedicated preambles inserted periodically within a pre-designated frame period. Preamble processing at the receiver provides initial estimates for the carrier phase, frequency and symbol timing within the incoming signal. During the data (payload) part of the frame, either decision-directed or pilot-based approaches are used (e.g., [8]) in order to refine, track and compensate these synch errors. This is all done at the receiver, without additional help from the transmitter. In transmitters with collocated antennas, the respective individual link variations tend to be correlated, thus not producing significant mutual variation within the composite channel. In a DBF setting, however, the intended remote receiver cannot possibly distinguish individual transmissions and thus track individual carrier offsets, because all emissions overlap in time and frequency (the distributed multiantenna paradigm). Furthermore, the channel variations produced by different distributed transmitters are clearly independent, resulting in significant variation. As a result, the individual errors can be viewed "free-running" within the frame and the system can only count on the start of the following synch frame for a new correction. This is what makes the composite DBF channel so prone to synch errors and channel variations.

It follows that the choice of the preamble length is critical: it must be chosen small enough to avert significant SNR loss due to synch-related plus channel-related misalignment, and yet not too small to avoid significant throughput loss due to the overhead associated with the per-frame preamble. In general, the frame length (t_{NF}) will be in the order of the coherence time of the composite effect.

We address here the DBF gain degradation due to these imperfections under the assumption that the *composite* channel is perfectly estimated and/or tracked at the receiver during the payload duration of the frame. A quantitative study of this degradation will then permit a good design of the synch and payload parts of the frame and thus determine the expected DBF gains of a given system. To quantify this gain we employ two specific performance metrics: the average transmission rate and the outage probability.

II. SYSTEM PERFORMANCE CHARACTERIZATION

A. Received signal model

Along the lines of the model in [3], the received signal $r(t)$ at a single-antenna DBF destination receiver (Rx) is the superposition of the channel-attenuated Tx signal $m(t)$, with receive signal-to-noise-ratio denoted as SNR, common to all $i = 1, \dots, N_{tx}$ transmitting radios, plus additive Gaussian Rx noise $n(t)$ with unit variance. We further assume a near-perfect time synch and a narrow-band channel model (i.e., a single complex-valued tap channel $g_i(t)$ for the i-th transmitter, with unit variance) plus we denote time measured in units of symbol duration T_s, i.e. $t = kT_s$; k=1,…, N_F. Then, $r(t)$ can be written as

$$r(t) = \left(\sum_{i=1}^{N_{tx}} w_i g_i(t) \mathrm{e}^{\mathrm{j}\varphi_i(t)} \right) m(t) + n(t) \qquad (1)$$

In (1), $\varphi_i(t)$ is the time-dependent phase rotation due to overall misalignment. There are various reasons for this phase misalignment, including oscillator phase error and random frequency offset. Specifically, we will model $\varphi_i(t)$ as $\varphi_i(t) = \omega_i t + \theta_i$, where the random cyclic frequency

offset $\omega_i = 2\pi f_i$ and the initial phase error θ_i are assumed to be independent and Gaussian distributed for each transmitter Tx*i*, with variances equal to $\sigma_\omega^2 = 4\pi^2\sigma_f^2$ and σ_θ^2, respectively, with σ_ω, σ_f, and σ_θ measured in rad-Hz, Hz and rad, respectively. Hence, the total variance of the random phase $\varphi_i(t)$ can be expressed as $\sigma_\varphi^2(t) = \sigma_\omega^2 t^2 + \sigma_\theta^2$. At the start of the synch frame it follows that $\varphi_i(0) = \theta_i$, i.e., the phase mismatch is only attributed to the initial phase estimation error, gradually changing with time due to the impact of the frequency error. Also, we let w_i be the beamforming weight applied at the *i*-th transmitter which, since each transmitter possesses information of solely its own channel at the beginning of the frame, takes the optimal form

$$w_i = \frac{g_i^*(0)}{|g_i(0)|} \tag{2}$$

The composite channel inside the parenthesis of (1) will produce a DBF gain which is a random process (r.p.) in time because, as we mentioned, both the channel gains $g_i(t)$ and the phases $\varphi_i(t)$ are time varying. The instantaneous receive power gain $P_R(t)$ at time *t* can then be expressed as

$$P_R(t) = \left\| \sum_{i=1}^{N_{tx}} w_i g_i(t) \mathrm{e}^{\mathrm{j}\varphi_i(t)} \right\|^2 \tag{3}$$

Since each transmitter is emitting at a given fixed power, the *total* nominal transmit power (namely, before any beamforming gains) is proportional to N_{tx}, the number of active transmitters. This is an important notational as well as architectural difference from [3] in that we are not normalizing the total Tx power among all transmitters, as is common in collocated transmit antenna systems; thus, there is no matched power loading per Tx (namely, the familiar g_i^*factor, resulting in the respective $|g_i|^2$ contribution to the Rx). This is a consequence of the fact that transmitters are spatially separated, each operating with its own transmit power constraint. Hence, in addition to the phase error $\varphi_i(t)$ gradually increasing, the phase coherence of $w_i g_i(t)$ also deteriorates with time as the channel decorrelates, resulting in gradually worsening beamforming gains.

Let N_F be the symbols per frame. Then, the time-averaged throughput in bits per channel use (bpcu) is

$$C = \frac{1}{N_F} \sum_{k=1}^{N_F} \log_2[1 + \mathrm{SNR}\, P_R(kT_s)] \tag{4}$$

When the SNR is very small (for example, in very long-haul transmission), the throughput C is approximately equal to an upper bound given by

$$C \le \frac{\mathrm{SNR}\, \bar{P}_R}{\ln 2} \tag{5}$$

where we define the average gain as

$$\bar{P}_R = \frac{1}{N_F} \sum_{k=1}^{N_F} P_R(kT_s) \tag{6}$$

It will be convenient to employ a tighter upper bound to the throughput (this will prove surprisingly tight over a wide range of SNR), namely

$$\bar{C} = \log_2[1 + \mathrm{SNR}\, \bar{P}_R] \ge C \tag{7}$$

To provide a statistical description for the throughput, we will employ two metrics. The first, which provides information on the average beamforming gains of a total link, is the ergodic capacity averaged over the frame duration, during which the beamforming gains may have changed. This is given by

$$E[C] = \frac{1}{N_F} \sum_{k=1}^{N_F} E[\log_2[1 + \mathrm{SNR}\, P_R(kT_s)]] \tag{8}$$

We will evaluate this metric by providing an accurate approximation for the distribution of $P_R(t)$. The second metric is the (uncoded) symbol error rate (SER) for 4QAM encoding, which is given by

$$SER = \frac{1}{N_F} \sum_{k=1}^{N_F} E\left[\mathrm{Q}\left(\sqrt{\mathrm{SNR}\, P_R(kT_s)}\right)\right] \tag{9}$$

where $Q(x) = \int_x^\infty \frac{dt\, e^{-\frac{t^2}{2}}}{\sqrt{2\pi}}$. Finally, the third metric is the outage capacity, namely the rate r_{out} for which the instantaneous throughput C is lower than r_{out} for a fixed (pre-set) probability p_{out}, namely

$$p_{out} = Prob(r_{out} \ge C) \tag{10}$$

Since this metric provides insight about the worst-case beamforming gains and hence is more relevant to low SNRs, we will replace it with an upper bound on r_{out}, namely $\bar{r}_{out} \ge r_{out}$, which is defined as

$$p_{out} = Prob(\bar{r}_{out} \ge \bar{C}) \tag{11}$$

We will in fact show that this lower bound is surprisingly tight for a wide range of small and medium SNRs.

B. DBF gain: moments

To address the statistics of the DBF gain, we start by evaluating its moments. To do so, in addition to the phase fluctuations statistics, we will need to characterize the fluctuations of the channel coefficients and their temporal correlations. Specifically, we will assume that the channel is complex Gaussian, independent between different transmitters with covariance given by

$$E[g(t)g^*(t')] = \rho(t - t') \tag{12}$$

with $\rho(0) = 1$. For concreteness, we will assume a specific form for $\rho(t)$, namely:

$$\rho(t) = e^{-\frac{(2\pi\sigma_d t)^2}{2}} \tag{13}$$

with $\sigma_d^2 = \frac{f_d^2}{2}$, and f_d being the usual Doppler spread in Hertz. With these assumptions, we prove in the Appendix that the first moment of the gain (namely, its mean) is given by

$$E[P_R(t)] = N_{tx}(1 + (N_{tx} - 1)|\mu_1(t)|^2 e^{-\sigma_\varphi^2(t)}) \tag{14}$$

Similarly (see Appendix), its covariance at different times is

$$E[P_R(t)P_R(t')] = \sum_{n=1}^{4} N_n \nu_n(t,t') \quad (15)$$

Expressions for N_n and $\nu_n(t,t')$ plus a short description of how they can be derived appear in the Appendix. Based on the above moments, we may also evaluate the moments of $\bar{P}_R$. Thus,

$$E[\bar{P}_R(t_F)] = N_{tx} + N_{tx}(N_{tx} - 1)\frac{1}{N_F}\sum_{k=1}^{N_F}|\mu_1(kT_s)|^2 e^{-\sigma_\varphi^2(kT_s)} \quad (16)$$

$$E\left[\bar{P}_R{}^2(t_F)\right] = \frac{1}{N_F^2}\sum_{m=1}^{N_F}\sum_{n=1}^{N_F}\sum_{k=1}^{4} N_k \nu_k(mT_s, nT_s) \quad (17)$$

We notice that the average power gain is maximized at t=0, whose value (in the absence of phase noise ($\sigma_\theta = 0$) is $E[P_R(0)] = N_{tx}(1 + (N_{tx} - 1)\frac{\pi}{4})$. This scales as N_{tx}^2 for large enough N_{tx}, while at large time scales it tends to $E[P_R] \to N_{tx}$. The characteristic time at which the DBF gain starts deviating significantly from $\sim N_{tx}^2$ occurs when the term $(N_{tx} - 1)|\mu_1(t)|^2 e^{-\sigma_\varphi^2(t)}$ becomes of order unity. For concreteness, then, we define the time t_{DBF} as to when this quantity equals ½. It is easy to prove that

$$t_{DBF} = \frac{\sqrt{\log\left(\frac{\pi}{2}(N_{tx} - 1)\right)}}{2\pi\sqrt{\sigma_d^2 + \sigma_f^2}} \quad (18)$$

We thus conclude that the both Doppler spread and the random-frequency-offset effect conflate together into a *single characteristic time scale*. We also notice that this time scale has a mild dependence on the number of antennas, pointing to the fact that it will take longer for larger arrays to lose their coherence. We expect this characteristic time scale to mark the transition in behavior for all moments of the power gain.

C. PDF fitting

Based on the moments evaluated in the previous Section, we will now fit a "synthetic" distribution to $P_R(t)$ and $\bar{P}_R$ which will provide a good approximation to the ergodic throughput and the outage capacity. To motivate this distribution, we look at the limit of a very long time, when the effective channel coherence evaporates. At this limit, the effective channel coefficients $w_i g_i(t) e^{j\varphi_i(t)}$ can be treated as a complex Gaussian r.v.; then, $P_R(t)$ tends to a χ^2-random variable with mean N_{tx}. Noting that the exponential distribution of a χ^2-variable is a special case of a Gamma variable, it is thus tempting to fit $P_R(t)$ with a hypothetical (approximate) Gamma distribution:

$$f(x) = \frac{\beta^\alpha x^{\alpha-1} e^{-\beta x}}{\Gamma(\alpha)} \quad (19)$$

Its shape α and rate β parameters can be obtained by matching the first two moments of the distribution given by (14) and (15) as follows:

$$a = \frac{E[x]^2}{E[x^2] - E[x]^2}, \beta = \frac{E[x]}{E[x^2] - E[x]^2} \quad (20)$$

It is then natural to hypothesize that $\bar{P}_R$ is well approximated by a Gamma, except using now the first two moments appearing in (16) and (17), respectively.

III. NUMERICAL RESULTS

We have mentioned the importance of choosing the preamble and frame lengths properly. The length of the first affects directly the residual synch (frequency/phase) errors. For a fixed preamble, the frame length determines the resulting DBF gain. A frame shorter than the coherence time (t_{DBF}) of the composite channel will produce large DBF gains while a frame longer than that will result in the mere non-coherent gain, which is always present. Here, we focus only on characterizing the system performance for a given set of length values. As a result, the relative length of the payload frame versus the coherence time will prove to be the most important parameter.

To showcase the analysis, we condition on several specific noise statistics values; however, under proper rescaling, these results can apply to any system under consideration as long as $T_s \ll t_{DBF}$. We consider two transmitter sets , $N_{tx} = 3$ and $N_{tx} = 10$. In addition, we take the initial frequency synchronization error to be σ_{f_0} =2Hz, whereas the initial phase error is $\sigma_\theta = 5^0$; the Gaussian Doppler spread is f_d = 5Hz. In Figure 1 we plot eq.(14) for these values, both by analysis (o) and simulation (.). The latter verifies the derivations but also demonstrates the importance of the defined coherence time t_{DBF} . For comparison, we also plot straight lines with average power gain $E[P_R] = N_{tx}$ which correspond to the completely incoherent limit. Finally, we also plot three other sub-cases error sources in order to illuminate the effect of each error source on the moments.

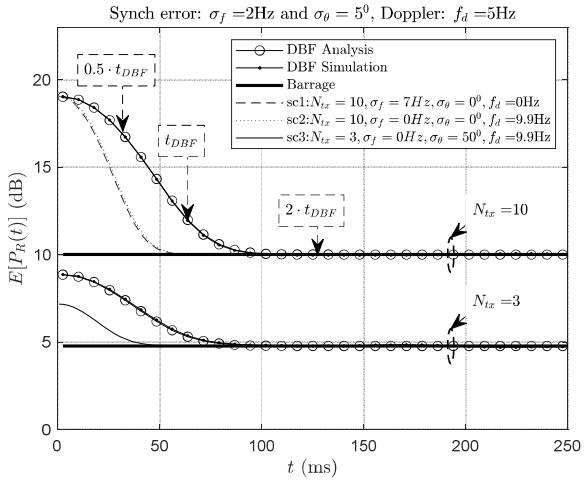

Figure 1: Symbol Mean of DBF gain; N_{tx} = [3,10].

This Figure above represents the first moment of the received SNR (scaled version) at different times within the received frame. The coherence at the start of the frame is naturally high since only the initial phase noise affects it negatively. As time marches on, the coherence gradually diminishes, since the other two sources of phase error, f_0 and f_d start to build up their effect. After a time period of a few t_{DBF}, the coherence

is totally lost and the first moment of the SNR has naturally converged to the incoherence case.

We will now test the approximation that the distribution of $P_R(t)$ is Gamma-distributed for various representative times, such as, at $t_0 = 0$, when coherence is full, at $t = 0.75 \cdot t_{DBF}$, and finally at $t = 2t_{DBF}$, for which coherence is completely lost. The three CDFs for each of the two antenna arrays are displayed in Figure 2. The empirical (simulated) CDF fits tightly the analytical CDF, not only in the incoherence region where it is naturally expected (χ^2), but also for the other two timescales. For the intermediate time t_{DBF}, we can notice a small difference for values lower than 10^{-1}. We focus on this small deviation by using the proposed distribution to compute the average capacity and the symbol rate.

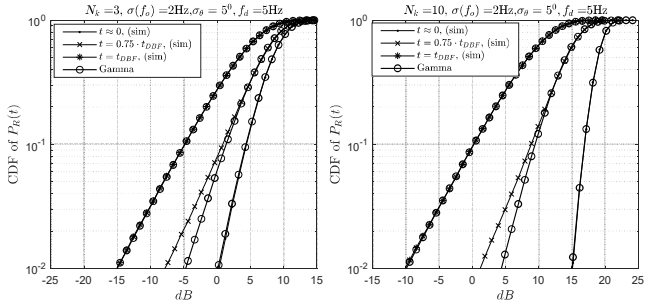

Figure 2: CDF of $P_R(t)$

We note that the average (ergodic) capacity of a Gamma variable can be expressed precisely via a well-known convolution property of Meijer-G functions (see eq 7.811 in [10]). Noting further that [11]

$$x^{\alpha}e^{-x} = G_{01}^{10}\left(\begin{matrix}-\\ \alpha\end{matrix}\middle| x\right)$$
$$\log_2(1+x) = G_{22}^{12}\left(\begin{matrix}1 & 1\\ 1 & 0\end{matrix}\middle| x\right) \quad (21)$$

we have

$$E[C] = \int_0^{\infty} \frac{\beta^{\alpha}x^{\alpha-1}e^{-\beta x}\log_2(1+\mathrm{SNR}\,x)\,dx}{\Gamma(\alpha)} = \frac{G_{32}^{13}\left(\begin{matrix}1-\alpha & 1 & 1\\ & 1 & 0\end{matrix}\middle| \frac{\mathrm{SNR}}{\beta}\right)}{\Gamma(\alpha)} \quad (22)$$

In Figure 3 we plot the analytical and simulated average capacity for different frame lengths t_{NF}. The two extreme cases are: (a) $t_{NF} = 0$, which corresponds to systems with $f_0 = f_d = 0$, (b) $t_{NF} = t_{DBF}$ for a system that has a frame within the order of coherence, and (c) $t_{NF} = 2 \cdot t_{BR}$ for a system which ends up deep within the non-coherence region. The average capacity of a non-coherent system with a frame length of $t_{NF} = 2 \cdot t_{BR}$ is also plotted to serve as the baseline system for assessing the gains of DBF.

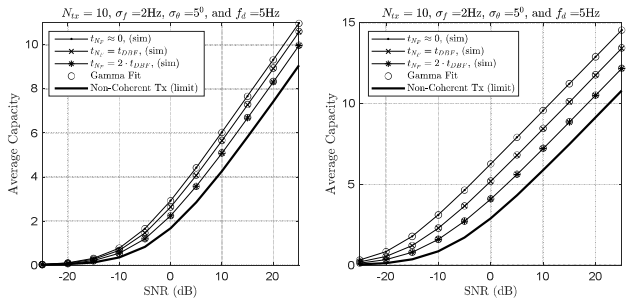

Figure 3: Average Capacity

The analysis agrees perfectly with the simulation for all cases of assumed frame lengths. We again stress the fact that t_{DBF} and its relation to the frame length is the one critical parameter which determines the resulting performance gain, always in comparison to the incoherent co-transmission.

Further, we compute the symbol error rate of a frame for a 4-QAM constellation by averaging the error rate within the frame. A closed formula is used for Gamma SNR (Nakagami fading) channels [9]. In Figure 4 we plot the simulated and analytic symbol error rate, again for various lengths of frames. The analysis deviates from simulation only when the frame length captures all the transition from coherence to incoherence, as expected. Even in those cases, it is very tight for all practical symbol error rates, (assuming the existence of a proper error correcting code in practical systems).

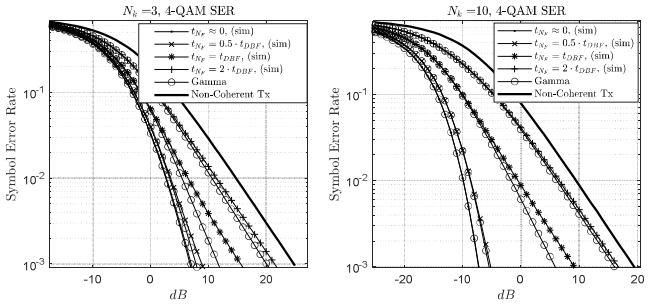

Figure 4:4-QAM symbol error rate

Another important consideration is the frame-outage statistics. As mentioned before, we will do this by comparing the outage capacity to the outage of $\bar{C}$ defined in (7). To do this we first need to demonstrate the accuracy of the Gamma-distribution for $\bar{P}_R$ in (6). In Figure 5 we demonstrate the appropriateness of the Gamma fit for eq. (6), where now $t_{NF} = 0, \mathrm{t_{DBF}}$ and $2 \cdot \mathrm{t_{DBF}}$.The curves demonstrate a close fit over 10^{-1} for a small number of transmit antennas, which gets tighter as the N_{tx} increases. For all cases the proposed statistics are demonstrably suitable as a tool for performance analysis.

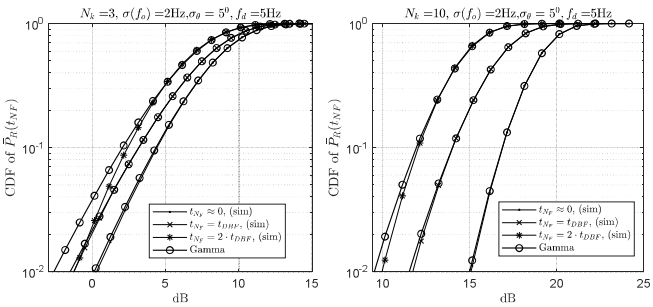

Figure 5: CDF of $\bar{P}_R$

Subsequently, in Figure 6 we plot the outage capacities for r_{out} and $\bar{r}_{out}$ for outage probability 5%, as defined in (10) and (11) respectively, noting again that in general $\bar{r}_{out} \geq r_{out}$. We plot the outage capacities for various frame-lengths for the same system parameters and include as well, for

comparison, the fully incoherent case. We find the agreement to be good for all times.

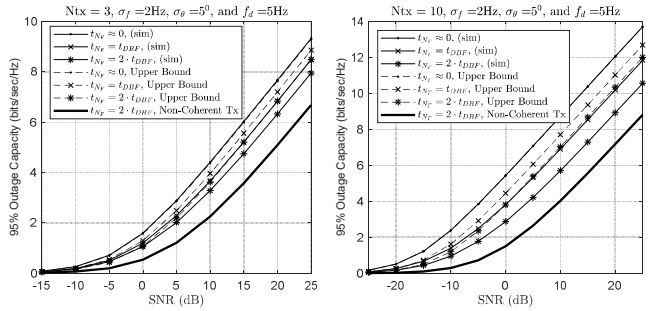

Figure 6: Outage Capacity and Upper Bound

IV. Conclusions

In conclusion, we have provided an analysis of performance due to various sources of error (imperfect synch, channel dynamics) in DBF-enabled networks. The computation is tedious but arrives at closed-form expressions. A Gamma-pdf approximation based on the derived moments yields a satisfactory approach for computing the requisite re-synch interval, which is the parameter of focus here. An extension of the theory would address the impact of statistically different individual link gains and would also compare open- versus closed-loop architectures from the standpoint of re-synch requirements (thus, indirectly, throughput loss).

Appendix A: First and Second DBF gain moments

A.1. Random Phase and Channel Statistics

To calculate the various moments of the received total power, we must compute the corresponding moments of the random phase offsets and channel coefficients. We start by noting that the averages over random variables of different transmitters factorize due to independence, and hence we will only deal with moments from a single transmitter.

The random phase has been modeled as $\varphi(t) = \omega t + \theta$, with ω and θ being zero-mean Gaussian random variables with variance σ_ω^2 and σ_θ^2 , respectively, and hence is Gaussian. Therefore, for $\epsilon_n = \pm 1$ and times t_n for $n = 1, \dots, z$ the following is true:

$$E\left[e^{j\sum_{n=1}^{z}\epsilon_n\varphi(t_n)}\right] = e^{-\frac{\sigma_\omega^2}{2}(\sum_{n=1}^{z}\epsilon_n t_n)^2 - \frac{\sigma_\theta^2}{2}(\sum_{n=1}^{z}\epsilon_n)^2} \quad (23)$$

To evaluate the moments of the channel coefficients, we will use the following identity:

$$E[g(t)F(\{g\},\{g^*\})] = \sum_{t'} E[g(t)g(t')^*]\, E\left[\frac{\partial F(\{g\},\{g^*\})}{\partial g(t')^*}\right] \quad (24)$$

The above formula is valid for any function $F(\{g\},\{g^*\})$ of complex Gaussian channel elements $g(t), g(t')$ at possibly different times, when the sum on the right-hand side is over all time instances for which $g(t')^*$ appears in the function, and under the condition that this function increases slower than the Gaussian distribution of the elements at $|g(t)| \to \infty$; furthermore, the expectations at both sides of the equation must be finite. This identity follows from Stein's Lemma and can be directly proved by integration by parts. Applying this formula several times, using the short-hand notation for the composite channel $h(t) = wg(t)$ and employing the expression for the cross-correlation for the channel $g(t)$ in (12), the following expressions can be derived:

$$\begin{aligned} \mu_1(t) &= E[h(t)] = \frac{\sqrt{\pi}}{2}\rho(t) \\ \mu_2(t,t') &= E[h^*(t)h(t')] = \rho(t-t') \\ \bar{\mu}_2(t,t') &= E[h(t)h(t')] = \rho(t)\rho(t') \\ \mu_3(t,t') &= E[|h(t)|^2 h(t')] \\ &= \Gamma\left(\frac{3}{2}\right)\left(\rho(t') + \rho(t)\rho(t'-t) - \frac{\rho(t')|\rho(t)|^2}{2}\right) \\ \mu_4(t,t') &= E[|h(t)|^2|h(t')|^2] \\ &= 1 + |\rho(t-t')|^2 \end{aligned} \quad (25)$$

A.2. First DBF gain moment

An expansion of (1) yields

$$\begin{aligned} &E[P_R(t)] \\ &= \sum_{k=1}^{N_{tx}} E[|h_k(t)|^2] \\ &+ \sum_{k=1}^{N_{tx}}\sum_{l=1,l\neq k}^{N_{tx}} E[h_k(t)h_l(t)^*]E[e^{j(\varphi_k(t)-\varphi_l(t))}] \end{aligned} \quad (26)$$

Direct application of (23) and (25) yields (14).

A.2. Second DBF moment

We will now outline the evaluation of the moment $E[P_R(t)P_R(t')]$. By expanding (3) and using the expression for the composite channel $h_i(t) = w_i g_i(t)$ we get

$$\begin{aligned} &E[P_R(t)P_R(t')] \\ &= \sum_{i_1,j_1,i_2,j_2=1}^{N_{tx}} E\left[h_{i_1,j_1,i_2,j_2}(t,t')\right]E[e^{j\varphi_{i_1,j_1,i_2,j_2}(t,t')}] \end{aligned} \quad (27)$$

where each term has two expectations for two independent r.v's. These two r.v's involved are defined as

$$h_{i,j,k,l}(t,t') = h_i(t)h_j^*(t)h_k(t')h_l^*(t') \quad (28)$$

and

$$\varphi_{i,j,k,l}(t,t') = \varphi_i(t) - \varphi_j(t) + \varphi_k(t') - \varphi_l(t') \quad (29)$$

The sum includes N_{tx}^4 different terms. However, due to the independence and identical distribution of the channels and phases of each transmitter, the averaging operation will provide a far smaller number of moments, which can be categorized by the multiplicity of indices that are equal with each other. The first set of

$$N_4 = \frac{\Gamma(N_{tx}+1)}{\Gamma(N_{tx}-3)} \quad (30)$$

index combinations include those with all different indices, where $\Gamma(x)$ is the usual Gamma function. This takes the value of $(x-1)!$ for positive integers and is infinite for non-positive integers. For this set, the corresponding moment can be shown to be

$$\nu_4(t,t') = |\mu_1(t)|^2|\mu_1(t')|^2 e^{-\sigma_\omega^2(t^2+t'^2)-2\sigma_\theta^2} \quad (31)$$

The second set of

$$N_3 = \frac{\Gamma(N_{tx}+1)}{\Gamma(N_{tx}-2)} \quad (32)$$

combinations include those with three distinct indices. In this case the moments are

$$\begin{aligned} \nu_3(t,t') &= |\mu_1(t)|^2 e^{-\sigma_\omega^2 t^2} + \left|\mu_1(t')\right|^2 e^{-\sigma_\omega^2 t'^2} + \\ &2\,Re\left[\mu_2(t,t')\mu_1(t)\mu_1(t')^*\right] e^{-\frac{\sigma_\omega^2}{2}\left((t-t')^2+t^2+t'^2\right)-\sigma_\theta^2} \\ &+2\,Re\left[\bar{\mu}_2^*(t,t')\mu_1(t)\mu_1^*(t')\right] e^{-\frac{\sigma_{f\omega}^2\left((t+t')^2+t^2+t'^2\right)}{2}-3\sigma_\theta^2} \end{aligned} \quad (33)$$

In the above expression the first two terms originate from combinations with $i_1 = j_1$ and $i_2 = j_2$, respectively, while the next two terms from combinations with $i_1 = j_1$ or $i_2 = j_1$ and $i_1 = i_2$ or $j_1 = j_2$ respectively. The third set of

$$N_2 = \frac{\Gamma(N_{tx}+1)}{\Gamma(N_{tx}-2)} \quad (34)$$

combinations include terms with two distinct indices, resulting to

$$\begin{aligned} &\nu_2(t,t') \\ &= 1 + |\bar{\mu}_2(t,t')|^2 e^{-\sigma_\omega^2 (t+t')^2 - 4\sigma_\theta^2} \\ &+ |\mu_2(t,t')|^2 e^{-\sigma_\omega^2 (t-t')^2} \\ &+ 2\,Re[\mu_3(t,t')\mu_1(t')] e^{-\sigma_\omega^2 t'^2 - \sigma_\theta^2} \\ &+ 2\,Re[\mu_3(t',t)\mu_1(t)] e^{-\sigma_\omega^2 t^2 - \sigma_\theta^2} \end{aligned} \quad (35)$$

Here, the constant term corresponds to $i_1 = j_1$ and $i_2 = j_2$, the second term corresponds to $i_1 = i_2$ and $j_1 = j_2$, the third term has $i_1 = j_2$ and $i_2 = j_1$, while the fourth term corresponds to $i_1 = j_1 = j_2$ and the last term has $i_2 = j_1 = j_2$. Finally, for the $N_1 = N_{tx}$ terms with all indices being equal, the moment expression is

$$\nu_1(t,t') = \mu_4(t,t') \quad (36)$$

V. Acknowledgment

This work was supported by the US Office of Naval Research through the Grand N62909-18-1-2141.

VI. References

[1] W. Lindsey, F. Ghazvinian, W. Hagmann and K. Dessouky, "Network Synch," *Proc. IEEE*, vol. 73, pp. 1445-1467, Oct. 1985.

[2] H. Ochiai, P. Mitran, H.V. Poor and V. Tarokh, "Collaborative beamforming for distributed wireless ad hoc sensor networks," *IEEE Trans. ASSP*, vol. 53, pp. 4110–4124, Oct. 2005.

[3] R. Mudumbai, G. Barriac and U. Madhow, "On the feasibility of distributed beam-forming in wireless networks," *IEEE Trans. Wireless Commun*., Vol. 6, pp. 1754-1763, May 2007.

[4] D. Brown III and H.V. Poor, "Time-slotted round-trip carrier synch for distributed beamforming," *IEEE Trans. Signal Processing*, vol. 56, pp. 5630-5643, Nov. 2008.

[5] B. Peiffer, R. Mudumbai, A. Kruger, A. Kumar and S. Dasgupta, "Experimental demonstration of a distributed antenna array pre-synchronized for retrodirective transmission," *Proc. CISS'16*, pp. 460–465, 2016.

[6] K. Alexandris, G. Sklivanitis and A. Bletsas, "Reachback WSN Connectivity: Non-Coherent Zero-Feedback Distributed Beamforming or TDMA Energy Harvesting?," *IEEE Trans. Wireless Commun.*, vol. 13, pp. 4923–4934, Sep. 2014.

[7] Wen-Qin Wang, "Carrier Frequency Synch in Distributed Wireless Sensor Networks," *IEEE Systems Journal*, pp. 703 – 713, July 2014.

[8] I. Dagres and A. Polydoros, "Decision-directed least-squares phase perturbation compensation in OFDM systems," *IEEE Trans. Wireless Commun.*, vol. 8, pp. 4784-4796, Sept. 2009.

[9] H. Shin and J. H. Lee, "On the error probability of binary and M-ary signals in Nakagami-m fading channels," *IEEE Trans. on Commun.*, vol. 52, no. 4, pp. 536-539, April 2004.

[10] I. S. Gradshteyn and I. M. Rezhik, "*Tables of Integrals, Series and Products*", 7th edition, Elsevier, Academic Press.

[11] G. Akemann, J. R. Ipsen and M. Kieburg, "Products of rectangular random matrices: Singular values and progressing scattering", *Phys. Rev.* E 88 (052118) 2013.